

MULTIPLE EQUILIBRIA FOR UNLINKED AND WEAKLY-LINKED CELLULAR STRUCTURAL FORMS

KIYOHIRO IKEDA

Department of Civil Engineering, Nagaoka University of Technology, Nagaoka,
Niigata 940-21, Japan

PAULO PROVIDÊNCIA†

Department of Civil Engineering, Universidade de Coimbra, Portugal

and

GILES W. HUNT

Department of Civil Engineering, Imperial College of Science, Technology and Medicine,
London SW7 2BU, U.K.

(Received 3 October 1991; in revised form 15 May 1992)

Abstract—It is demonstrated that a structural form comprising n unlinked or weakly-linked separate identical cells can, by its nature, suffer an explosion of unstable post-buckling states, associated with an n -fold compound critical point. Examples of rigid-link models, and atomic matrix cellular models employing a Lennard–Jones potential, are included. Attention is paid to criteria for the appearance of homogeneous, localized but distributed, and thoroughly-localized solutions. For the atomic models, generalized coordinates that exploit local and global symmetries of unlinked cells are introduced in a block diagonalization context, to clarify the bifurcation structure. A discretized Lagrangian formulation is introduced to untangle the paths for weakly-linked cells.

1. INTRODUCTION

There are many structural and structural-like systems that are quite naturally represented as a sequence of unlinked or weakly-linked cells (Born and Huang, 1954; Macmillan and Kelly, 1972; Thompson and Shorrock, 1975). Consider, for example, the two cases in Fig. 1(a). Above we have a set of n separate compressed initially-flat rigid-bar and spring elements, connected in series and extended at both ends. Below is a schematic representation of a stressed two-dimensional array of atoms, held together by a Lennard–Jones or some such energy potential; these are usefully represented by balls rolling on one another, in recognition of the extremely stiff nature of the initial atomic bond. In each case, since there is no energy transfer between cells, the energy of the total structure is simply made up of the sum of the individual cell energies.

If, however, cells are linked, as shown in Fig. 1(b), there is room for energy transfer across boundaries between cells; there are now cross-terms linking cell deflections, and the whole energy is not merely the sum of the individual parts. In the spirit of the energy approach, a discrete-coordinate Lagrangian formulation is suggested for such problems (Hunt *et al.*, 1992), which is able to reflect the differential equation of a continuous system.

The disconnected cellular structure of the unlinked case gives special properties to the energy functions, due to the local symmetry for each cell and the hidden global symmetry for the whole structure. The local symmetry is exploited by block diagonalization (Dinkovich, 1991; Murota and Ikeda, 1991; Ikeda and Murota, 1991; Healey and Treacy, 1991), which usually relates to quadratic terms of energy, but can be extended to cubic and higher-order terms (Miller, 1972). The hidden global symmetry is clarified by a simple coordinate transformation which removes rigid-body displacement. A theory is developed to deal with critical states on a primary loading path, it being demonstrated that such states, which are by their very nature n -fold compound critical, can be either limit points or bifurcation points (Thompson and Hunt, 1984). With linking among cells, this n -fold criticality decomposes into n discrete critical points on the primary path, surrounded by a plethora of

† Present address: Department of Civil Engineering, Imperial College, London, U.K.

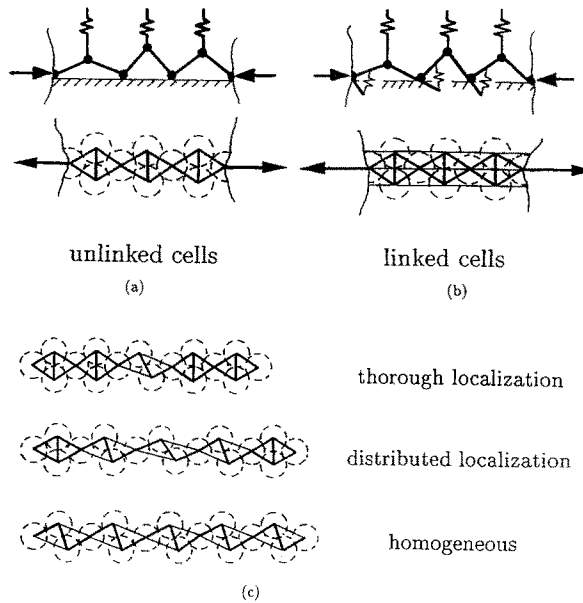


Fig. 1. (a) Unlinked models; (b) Weakly-linked models; (c) Various kinds of localization.

secondary bifurcations and a consequential cascade of possible post-buckling solutions (Hunt, 1989).

The new theory for unlinked cells is applied to the atomic lattice problem with the well-known Lennard-Jones potential representing initial interatomic forces, and “broken” atomic bonds (with the balls well-separated) ignored. The critical state is found to be one of n -fold bifurcation on the rising primary path, met before any limit point is reached. The paper goes on to speculate on possible solutions when linking is present between cells. Three possible different forms of deformation of the cells after bifurcation, resulting from different linking properties, are given in Fig. 1(c).

2. LAGRANGE THEORY FOR RIGID-BAR MODEL

For the “perfect” unlinked rigid-bar model at the top of Fig. 1(a), in which all springs are unstressed in the entirely flat (fundamental) equilibrium state, it is a simple matter to show that thoroughly localized solutions are preferred. For cells in series, the global stiffness is obtained by summing up local stiffnesses according to a reciprocal relation (Hunt, 1989), and hence if post-critical paths fall with respect to load (negative stiffness), a thoroughly localized response is the least stiff, as seen at the bottom of Fig. 2; this also means that it has the minimum triggering energy requirement, when held at a subcritical load (Hunt *et al.*, 1989).

If we introduce an amplitude function

$$a_i = (-1)^{i+1} Q_i,$$

where Q_i is defined as in Fig. 3, and a corresponding rate of change of amplitude,

$$v_i = a_{i+1} - a_i, \quad (1)$$

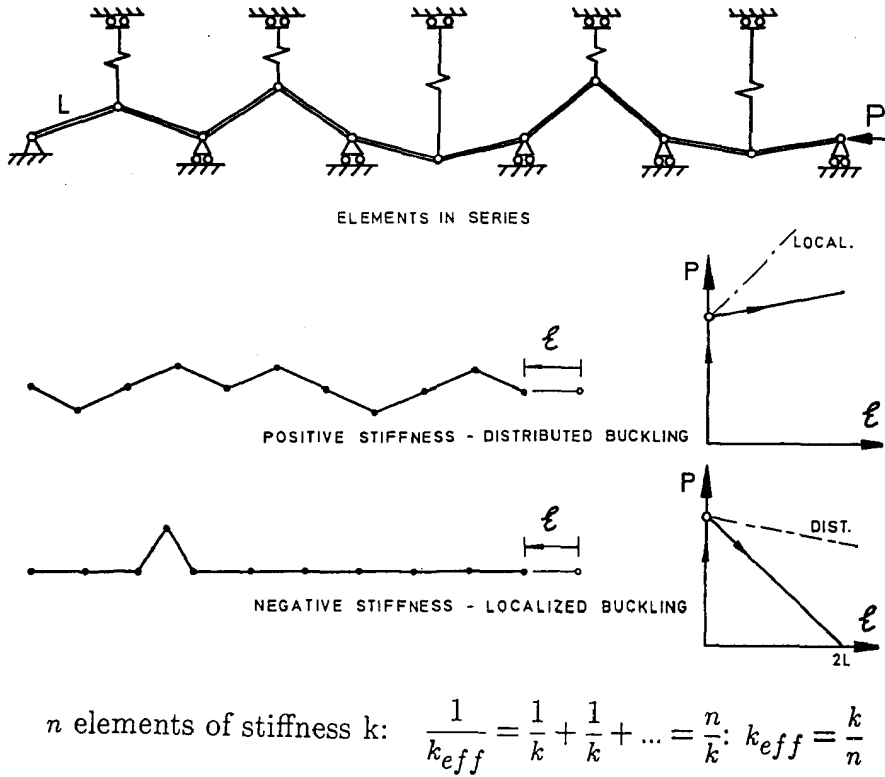


Fig. 2. Responses of unlinked rigid-bar models [see Hunt (1989)].

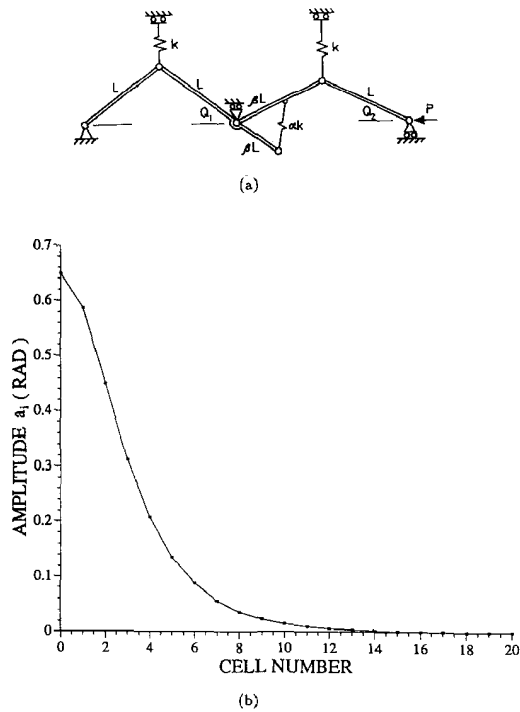


Fig. 3. Linked rigid bar model. (a) Definition of rotational displacements Q_i ($n = 2$); (b) Localized solution at $P = 0.9P^c$, $c = 1$.

a discrete-coordinate version of the Lagrange equation appears. With no linking between cells, the total energy of the system is simply the sum of individual cell energies :

$$V_{\text{unlinked}} = \frac{kL^2}{2} \sum_{i=1}^n \sin^2 a_i - 2PL \sum_{i=1}^n (1 - \cos a_i),$$

and the total potential energy is diagonalized with n identical entries prior to buckling (Thompson and Hunt, 1973); the critical point of the system thus becomes an n -fold compound.

If cells are linked, however, as in Fig. 3, such that the extra springs are unstressed in the periodic state, $a_i = a_{i+1}$ ($Q_i = -Q_{i+1}$), the deflection in the general linking spring is then $2(-1)^i \beta L \sin(v_i/2)$ (Hunt, 1989), and summing the contributions gives

$$V_{\text{linking}} = ckL^2 \sum_{i=1}^{n-1} \sin^2 \left(\frac{v_i}{2} \right),$$

where $c = 2\alpha\beta^2$. Total energy is now given by $V_{\text{total}} = V_{\text{unlinked}} + V_{\text{linking}}$, and, after substituting for v_i from eqn (1), we find that the diagonalized property is lost; this decomposes the n -fold bifurcation into n distinct bifurcations on the primary path.

We can apply Lagrange multipliers λ_i to the constraint condition (1) to give the new potential energy function

$$\bar{V}_{\text{total}} = V_{\text{unlinked}} + V_{\text{linking}} + \sum_{i=1}^{n-1} \lambda_i (v_i - a_{i+1} + a_i).$$

Setting the derivative with respect to the new generalized coordinate v_i (away from the ends) to zero, gives

$$\lambda_i = - \frac{ckL^2}{2} \sin v_i,$$

and similarly setting the derivative with respect to a_i to zero then provides a general governing equation

$$- \frac{ckL^2}{2} (\sin v_i - \sin v_{i-1}) + \frac{\partial V_{\text{unlinked}}}{\partial a_i} = 0. \tag{2}$$

If we define a local Lagrangian function \mathcal{L}^i (for the i th cell) by

$$\sum_{i=1}^n \mathcal{L}^i = -V_{\text{total}} = -V_{\text{linking}} - V_{\text{unlinked}}, \tag{3}$$

where

$$\mathcal{L}^i = T(v_i) - V(a_i, P),$$

we can identify a discrete-coordinate spatial kinetic energy component

$$T^i = T(v_i) = -ckL^2 \sin^2 \left(\frac{v_i}{2} \right),$$

which is negative-definite; this is analogous to the positive-definite kinetic energy of Newtonian dynamics. The potential energy component of the Lagrangian is the *local* form of the unlinked case (with the summation sign removed),

$$V^i = V(a_i, P) = \frac{1}{2}kL^2 \sin^2 a_i - 2PL(1 - \cos a_i).$$

We can then recognize the governing equation (2) as a finite difference version of the Lagrange equation

$$\frac{d}{dX} \left(\frac{\partial \mathcal{L}^i}{\partial \dot{a}_i} \right) - \frac{\partial \mathcal{L}^i}{\partial a_i} = \frac{d}{dX} \left(\frac{\partial T^i}{\partial \dot{v}_i} \right) + \frac{\partial V^i}{\partial a_i} = 0,$$

in which a dot denotes a differentiation with respect to the spatial dimension X .

As $n \rightarrow \infty$ the significance of the ends disappears; of greater importance is the symmetric section, $v_i = 0$, from which forward and backward runs give the same response with the direction of X reversed. The amplitude of a distributed localized response is plotted from the symmetric section at the bottom of Fig. 3, with the value of $c = 1$ at $P = 0.9P^c$ (where $P^c = kL/2$ is the critical load). For models of finite length, end conditions must be satisfied, and a localized solution no longer develops smoothly out of the critical eigenvector; secondary bifurcations are now crucially involved, as seen in the $n = 2$ analysis of Hunt (1989).

3. BLOCK DIAGONALIZATION IN AN ATOMIC MATRIX

It is clear from the rigid-bar model of the previous section that the breaking of diagonalization with intercellular linking is a key phenomenon. It provides the mechanism, for example, for decomposing the n -fold bifurcation into n distinct critical points on the primary path, each with its own zero eigenvalue and corresponding eigenvector distributed over the length of the structure. For the atomic matrix model which follows, each cell has five independent degrees of freedom. The fully diagonalized property of the previous section thus becomes one of *block diagonalization* due to the “local” symmetry of each cell, to a base number of five. Linking between cells then breaks the “global” symmetry of the whole structure, again decomposing an n -fold bifurcation into n distinct eigenvalues and giving rise to the possibility of the distributed form of localization.

3.1. Unlinked cellular model

For the unlinked cellular model, shown in the bottom of Fig. 1(a), we ignore weak (or broken) atomic bonds between cells, corresponding to well-separated balls. Subject to axial force P at both ends, this exhibits a thoroughly localized bifurcation. In order to prevent rigid-body translation, both ends are assumed to displace the same amount in opposite directions. Each cell is made up of four atoms which are connected to each other with five interatomic forces (nonlinear elastic springs), as shown in Fig. 4. These forces are given as a function of the distance between atoms by the Lennard–Jones constitutive law for interatomic potentials (Macmillan and Kelly, 1972), among many other alternative forms.

3.1.1. *Local symmetry.* Each cell of the model in uniform deformation has the same “local” geometric symmetry, characterized by a diamond shape. In group-theoretic bifurcation theory, this symmetry is termed as an invariance with respect to the dihedral group D_2 of degree two†; the bifurcation behavioral characteristics of a D_2 -invariant system have been fully investigated [see e.g. Golubitsky and Schaeffer (1985) and Ikeda *et al.* (1991)].

The group D_2 , which consists of four geometric transformations, is defined as

$$D_2 = \{e, r, s, sr\},$$

where e is the identity transformation that leaves everything unchanged; r is the half rotation in the XY -plane around the center of the i th cell; s is the reflection with respect to the horizontal XZ -plane; sr is the reflection with respect to the vertical plane which

† In the Schoenflies notation this group is denoted as C_{2v} , while D_2 means another group.

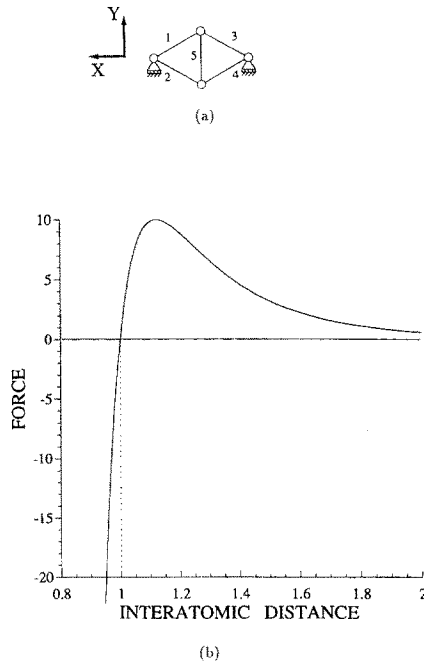


Fig. 4. (a) Definition of five interatomic forces (nonlinear springs); (b) Lennard-Jones constitutive law for interatomic potentials.

contains the center of the *i*th cell and is parallel to *YZ*-plane. This group has the following four subgroups, which represent the partial symmetry of D_2 :

$$C_2 = \{e, r\}, \quad D_1^1 = \{e, s\}, \quad D_1^2 = \{e, sr\}, \quad C_1 = \{e\},$$

where C_2 denotes deformation modes which are invariant with respect to the half rotation; D_1^1 indicates the modes invariant with respect to the reflection in the horizontal plane; D_1^2 expresses the modes invariant with respect to the reflection in the vertical plane; C_1 denotes asymmetric modes. Each of these groups labels the symmetry of the primary or bifurcation path of a D_2 -invariant system, and indicates that its bifurcation structure can be known *a priori* by the subgroup structure of D_2 shown in Fig. 5.

3.1.2. *Global symmetry.* The unlinked cellular model is invariant with respect to the action of the symmetric group S_n of degree *n*, which rearranges some or all of the *n* cells through permutation. This invariance is far more restrictive than that of the dihedral group which denotes the regular polygonal symmetry for shell structures [see e.g. Ikeda *et al.* (1991)]. This model, the “global” symmetry of which is characterized by the group S_n , will display far more complex and completely different bifurcation behavior than shell structures.

As a result of the local and the global symmetries, the model, to be precise, is $S_n \times D_2$ -invariant, where (\times) denotes the tensor product of groups. In this paper a simple local transformation is used to investigate its bifurcation behavior, whereas a more rigorous mathematical study, for example, can be found in Miller (1972).

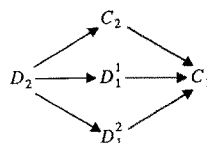


Fig. 5. Subgroup structure of D_2 expressing the bifurcation structure of each cell.

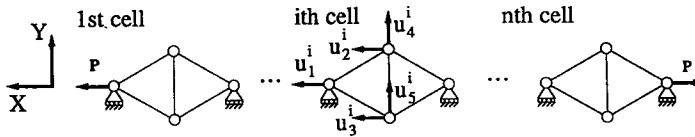


Fig. 6. Nodal displacements for unlinked cellular model made up of n identical cells.

3.1.3. *Local transformation.* We partition the displacement vector \mathbf{u} into n components $\mathbf{u}^i = (u_1^i, \dots, u_5^i)^t$ ($i = 1, \dots, n$) for cells, as shown in Fig. 6, that is,

$$\mathbf{u} = [(\mathbf{u}^1)^t, \dots, (\mathbf{u}^n)^t]^t,$$

where $(\cdot)^t$ denotes the transpose of a vector or matrix. Since for this coordinate system, strain energies of the $(i-1)$ th and the i th cells are both functions in u_1^i , the tangent stiffness matrix, and hence equilibrium equations, formulated in terms of \mathbf{u} will display interaction between cells. Further, the work done by load $2Pu_1^i$ belongs only to the end cells, and hence is not evenly distributed.

Such interaction and inequality between cells, in reality, are misleading and can be easily avoided by means of an appropriate local transformation :

$$\mathbf{u} = H\mathbf{q} = \sum_{i=1}^n H^i \mathbf{q}^i, \tag{4}$$

which exploits the “local” symmetry of each cell, and makes the “global” symmetry transparent by taking rigid body displacements of other cells into consideration. Here generalized coordinates \mathbf{q} and a local transformation matrix H consist of n vectors $\mathbf{q}^i = (q_1^i, \dots, q_5^i)^t$ and n submatrices $H^i = [\mathbf{h}^1, \dots, \mathbf{h}^5]$, respectively, that is,

$$\mathbf{q} = [(\mathbf{q}^1)^t, \dots, (\mathbf{q}^n)^t]^t, \quad H = [H^1, \dots, H^n].$$

Column vectors \mathbf{h}_j^i ($j = 1, \dots, 5$) for the i th cell, shown in Fig. 7, are given by

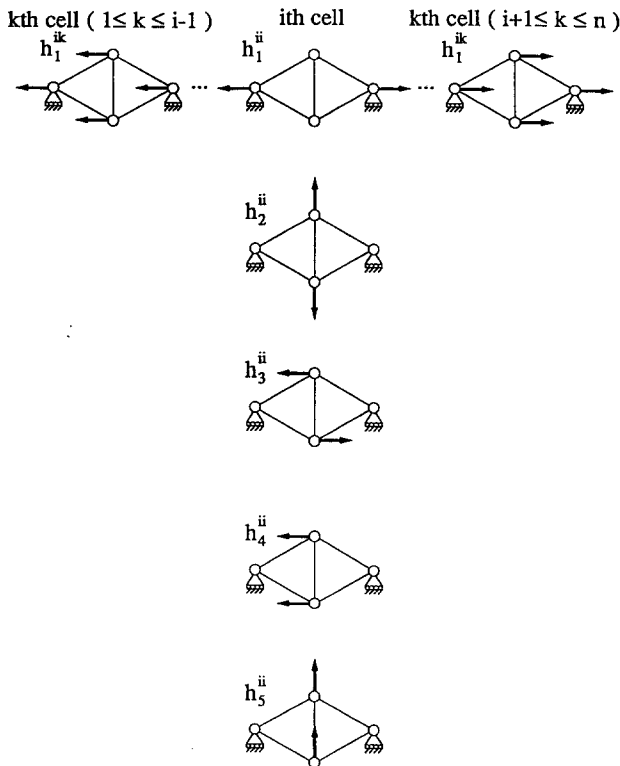


Fig. 7. Basis vectors \mathbf{h}^k forming local transformation matrix H .

$$\mathbf{h}_j^i = [(\mathbf{h}_j^i)^1, \dots, (\mathbf{h}_j^i)^n]^t,$$

where

$$\mathbf{h}_1^{ik} = \begin{cases} (1, 1, 1, 0, 0)^t, & k = 1, \dots, i-1, \\ (1, 0, 0, 0, 0)^t, & k = i, \\ -(1, 1, 1, 0, 0)^t, & k = i+1, \dots, n, \end{cases}$$

$$\mathbf{h}_2^{ik} = \delta_{ik}(0, 0, 0, 1, -1)^t, \quad \mathbf{h}_3^{ik} = \delta_{ik}(0, 1, -1, 0, 0)^t,$$

$$\mathbf{h}_4^{ik} = \delta_{ik}(0, 1, 1, 0, 0)^t, \quad \mathbf{h}_5^{ik} = \delta_{ik}(0, 0, 0, 1, 1)^t,$$

and in which δ_{ik} is Kronecker's delta. The vector \mathbf{h}_1^i denotes a horizontal expansion mode of the i th cell, accompanied with rigid-body displacement of the remaining $n-1$ cells; the other four vectors \mathbf{h}_j^i ($j = 2, \dots, 5$) denote deformation modes of only the i th cell. The vectors \mathbf{h}_1^i and \mathbf{h}_2^i are related to the most-uniform and most-symmetric modes for the primary path, and \mathbf{h}_j^i ($j = 3, 4, 5$) to symmetry-breaking bifurcation modes.

The total potential energy function \mathbf{V} of the model in the coordinate \mathbf{q} reads

$$\mathbf{V}(\mathbf{q}, P) = \sum_{i=1}^n V(\mathbf{q}^i, P),$$

where

$$V(\mathbf{q}^i, P) = U(\mathbf{q}^i) - Pq_1^i \quad (5)$$

is the total potential energy stored in the i th cell; $U(\mathbf{q}^i)$ expresses its strain energy; and Pq_1^i denotes its work done by load. The total potential energy $V(\mathbf{q}^i, P)$ of the i th cell, which is a function only in its displacement \mathbf{q}^i , is completely unlinked to adjacent cells; moreover, the same functional form is displayed for all cells. Independence and equality of cells, and hence the hidden global symmetry, have been fully clarified by the local transformation (4).

A number of derivatives of \mathbf{V} vanish systematically owing to the "local" symmetry of the model. The geometric transformations associated with the elements of D_2 act on the increment $\delta\mathbf{q}^i = (\delta q_1^i, \dots, \delta q_5^i)^t$ at an equilibrium point (\mathbf{q}, P) on the primary path such that

$$e(\delta q_j^i) = \delta q_j^i, \quad j = 1, \dots, 5; \quad r(\delta q_j^i) = \begin{cases} \delta q_j^i, & j = 1, 2, 3, \\ -\delta q_j^i, & j = 4, 5; \end{cases} \quad (6)$$

$$s(\delta q_j^i) = \begin{cases} \delta q_j^i, & j = 1, 2, 4, \\ -\delta q_j^i, & j = 3, 5; \end{cases} \quad sr(\delta q_j^i) = \begin{cases} \delta q_j^i, & j = 1, 2, 5, \\ -\delta q_j^i, & j = 3, 4. \end{cases} \quad (7)$$

The modes δq_1^i and δq_2^i are necessarily D_2 -invariant by eqns (6) and (7). Only partial symmetry of D_2 is retained for the modes δq_j^i ($j = 3, 4, 5$), which are invariant with respect to C_2 , D_1^1 , and D_1^2 , respectively.

The incremental form of \mathbf{V} is expressed as

$$\delta\mathbf{V} \equiv \mathbf{V}(\mathbf{q} + \delta\mathbf{q}, P + \delta P) - \mathbf{V}(\mathbf{q}, P) = \sum_{i=1}^n \delta V(\delta\mathbf{q}^i, \delta P). \quad (8)$$

For the primary path, each cell is D_2 -invariant, and hence \mathbf{V} is also invariant with respect to the transformations $\delta q_j^i \rightarrow -\delta q_j^i$ ($j = 3, 4, 5$) by eqns (6) and (7) [cf. Hunt (1986)]. Therefore $\delta V(\delta\mathbf{q}^i, \delta P)$ shows the following form:

$$\begin{aligned} \delta V(\delta \mathbf{q}^i, \delta P) = & \sum_{j=1}^2 \sum_{k=1}^2 \delta q_j^i \delta q_k^i \left(\frac{1}{2!} V_{jk} + \frac{1}{3!} \sum_{l=1}^2 V_{jkl} \delta q_l^i + \frac{1}{4!} \sum_{l=1}^2 \sum_{m=1}^2 V_{jklm} \delta q_l^i \delta q_m^i \right) \\ & + \frac{1}{2!} \sum_{j=3}^5 (\delta q_j^i)^2 \left(V_{jj} + \sum_{k=1}^2 V_{jjk} \delta q_k^i + \frac{1}{2} \sum_{k=1}^2 \sum_{l=1}^2 V_{jjkl} \delta q_k^i \delta q_l^i \right) \\ & + \frac{1}{4!} \sum_{j=3}^5 \sum_{k=3}^5 (3 - 2\delta_{jk}) V_{jjkk} (\delta q_j^i)^2 (\delta q_k^i)^2 - \delta q_1^i \delta P + \text{h.o.t.}, \quad (9) \end{aligned}$$

in which h.o.t. denotes higher order terms, and the subscripts j, k, l and m of V denote partial differentiation with respect to q_j, q_k, q_l and q_m , respectively. Four diagonal blocks $\{V_{jk} | j, k = 1, 2\}$ and $V_{jj} (j = 3, 4, 5)$ have appeared for quadratic terms.

Setting the derivatives of eqn (8) with respect to δq_j^i to be zero yields $5 \times n$ incremental equations of equilibria. Note that the independence of the cells divides these equations into n different sets, and that the identical block-diagonal structure of each cell subdivides each set into four subsets, respectively. There consequently exist a total of $4 \times n$ independent systems of equations, including: a set of n two-dimensional incremental equations:

$$\sum_{k=1}^2 J_{jk} \delta q_k^i - \delta_{1j} \delta P + \text{h.o.t.} = 0, \quad j = 1, 2, i = 1, \dots, n, \quad (10)$$

for the primary uniform solution, which display quadratic cross-terms between q_1 and q_2 , and three sets of n one-dimensional incremental equations:

$$\delta q_j^i (V_{jj} + \text{h.o.t.}) = 0, \quad j = 3, 4, 5, i = 1, \dots, n, \quad (11)$$

for symmetry-breaking bifurcated solutions with no such cross-terms. Here

$$J = \{J_{ij} | i, j = 1, 2\} = \{V_{ij} | i, j = 1, 2\}$$

indicates a 2×2 tangent stiffness matrix for the primary path. The symmetry of the model for the primary path has thus been fully exploited, while retaining complete information on bifurcated solutions.

Because J and $V_{jj} (j = 3, 4, 5)$ appear in n different equations, each critical point on the primary path is necessarily n -fold compound. Possible equilibrium states on the primary path include (1) ordinary points, (2) n -fold compound limit points, and (3) n -fold compound points of bifurcation. Characteristics of these points are explained in the following subsections.

3.1.4. Ordinary points. For an ordinary point on the primary path, the tangent stiffness matrix J in eqn (10) is nonsingular and the stability coefficients $V_{jj} (j = 3, 4, 5)$ in eqn (11) are all nonzero. Equation (11) then yields trivial solutions,

$$\delta q_3^i = \delta q_4^i = \delta q_5^i = 0, \quad i = 1, \dots, n,$$

whereas a set of n equations (10) yields the same solution for all cells,

$$\begin{pmatrix} \delta q_1^i \\ \delta q_2^i \end{pmatrix} = J^{-1} \begin{pmatrix} \delta P \\ 0 \end{pmatrix}, \quad i = 1, \dots, n, \quad (12)$$

which is D_2 -invariant. Thus each cell stores the same amount of total potential energy by eqn (5). A superposition of the solutions (12) with the use of eqn (4) leads to an incremental solution for uniform deformation

$$\delta \mathbf{u} = \left(\sum_{i=1}^n [\mathbf{h}_1^i, \mathbf{h}_2^i] \right) J^{-1} \begin{pmatrix} \delta P \\ 0 \end{pmatrix}.$$

3.1.5. *n-fold compound limit point.* The same matrix J in a set of n equations (10) becomes simultaneously singular at an n -fold compound limit point. Define at this point principal coordinates Q_j^i ($j = 1, \dots, 5$; $i = 1, \dots, n$) by

$$\begin{pmatrix} \delta Q_1^i \\ \delta Q_2^i \end{pmatrix} = [\mathbf{e}_1, \mathbf{e}_2]^{-1} \begin{pmatrix} \delta q_1^i \\ \delta q_2^i \end{pmatrix};$$

$$\delta Q_j^i = \delta q_j^i, \quad j = 3, 4, 5,$$

where \mathbf{e}_1 is the unit critical eigenvector of J such that $J\mathbf{e}_1 = 0$, and \mathbf{e}_2 is a unit eigenvector orthonormal to \mathbf{e}_1 . The Lyapunov-Schmidt decomposition (Sattinger, 1979) of eqns (10) and (11) results in the following set of n bifurcation equations:

$$(\delta Q_1^i)^2 - \alpha \delta P + \text{h.o.t.} = 0, \quad i = 1, \dots, n, \quad (13)$$

where

$$\alpha = -2 \left(\frac{\partial^2 V^i}{\partial P \partial Q_1^i} \right)^c \bigg/ \left(\frac{\partial^3 V^i}{\partial Q_1^3} \right)^c$$

is a constant independent of i , owing to the equality of the cells; and $(\cdot)^c$ denotes a value at a critical point. Equation (13) yields a pair of asymptotic solutions

$$\delta Q_1^i = \pm (\alpha \delta P)^{1/2} + \text{h.o.t.}, \quad i = 1, \dots, n,$$

also independent of i . The solution $\delta Q_1^i = -(\alpha \delta P)^{1/2}$ corresponds to the state of unloading down the original path, and $\delta Q_1^i = (\alpha \delta P)^{1/2}$ to that of softening.

Since each of the n cells can independently choose either the state of unloading or softening, a total of 2^n different paths (states of equilibria) asymptotically exist in the neighborhood of the n -fold compound limit point. Two correspond to the primary path in the states of unloading and softening, respectively; and remaining $2^n - 2$ to bifurcation paths. It is to be noted that bifurcation paths with the same number of cells in the state of unloading are quite similar in that they display the same external load P versus end displacement u_1^i relationship. Those $2^n - 2$ bifurcation paths, accordingly, are to be divided into $n - 1$ "physically independent" paths depending on the number of cells in the state of unloading. In the remainder of this paper, we count the number of bifurcation paths by means of the "physically independent" ones.

3.1.6. *n-fold compound point of bifurcation.* The incremental equation (11) has nonzero solution δq_j^i ($j = 3, 4, 5$) only at the n -fold compound point of bifurcation where one of the stability coefficients V_{jj} ($j = 3, 4, 5$) vanishes. A set of n critical eigenvectors expresses C_2 -invariant horizontal-shearing, D_1^1 -invariant horizontal-pulling out, or D_1^2 -invariant vertical-shearing motion of the i th cell ($i = 1, \dots, n$), according to whether $j = 3, 4$ or 5 . Each cell can choose independently either the state of bifurcation or nonbifurcation; accordingly, a total of n (physically independent) bifurcation paths branch at this point.

Consider a typical bifurcation path for which the first N cells are in the state of C_2 -invariant bifurcation mode, associated with δq_3^i , and the remaining $n - N$ cells in that of D_2 -invariant deformation. The state of these $n - N$ cells is described again by eqns (10) and (11), while that of the first N cells is investigated below.

We focus on the i th cell ($1 \leq i \leq N$) in the state of bifurcation with C_2 -invariant deformation. By eqn (6) its total potential energy $V(\mathbf{q}^i, P)$, which is also C_2 -invariant, must remain unchanged with respect to a transformation:

$$\begin{pmatrix} \delta q_4^i \\ \delta q_5^i \end{pmatrix} \rightarrow - \begin{pmatrix} \delta q_4^i \\ \delta q_5^i \end{pmatrix}.$$

The increment $\delta V(\mathbf{q}^i, P)$ of this cell, therefore, takes a special form :

$$\begin{aligned} \delta V(\mathbf{q}^i, P) = & \sum_{j=1}^3 \sum_{k=1}^3 \delta q_j^i \delta q_k^i \left(\frac{1}{2!} V_{jk} + \frac{1}{3!} \sum_{l=1}^3 V_{jkl} \delta q_l^i + \frac{1}{4!} \sum_{l=1}^3 \sum_{m=1}^3 V_{jklm} \delta q_l^i \delta q_m^i \right) \\ & + \frac{1}{2!} \sum_{j=4}^5 \sum_{k=4}^5 \delta q_j^i \delta q_k^i \left(V_{jk} + \sum_{l=1}^3 V_{jkl} \delta q_l^i + \frac{1}{2} \sum_{l=1}^3 \sum_{m=1}^3 V_{jklm} \delta q_l^i \delta q_m^i \right) \\ & + \frac{1}{4!} \sum_{j=4}^5 \sum_{k=4}^5 \sum_{l=4}^5 \sum_{m=4}^5 V_{jklm} \delta q_j^i \delta q_k^i \delta q_l^i \delta q_m^i - \delta q_1^i \delta P + \text{h.o.t.} \quad (14) \end{aligned}$$

In association with a partial loss of symmetry due to bifurcation, eqn (14) has more nonzero derivatives of V than eqn (9) for the primary path.

The increment of V thus displays a block-diagonal form among quadratic terms, with two diagonal blocks $\{V_{jk} | j, k = 1, 2, 3\}$ and $\{V_{jk} | j, k = 4, 5\}$. Incremental equilibrium equations, accordingly, are decomposed into those for the primary path and initial bifurcation eigenvector

$$\sum_{k=1}^3 V_{jk} \delta q_k^i - \delta_{1j} \delta P + \text{h.o.t.} = 0, \quad j = 1, 2, 3, i = 1, \dots, N,$$

the solution of which is C_2 -invariant, and those associated with secondary bifurcations

$$\sum_{k=4}^5 V_{jk} \delta q_k^i + \text{h.o.t.} = 0, \quad j = 4, 5, i = 1, \dots, N,$$

the solution of which is asymmetric (C_1 -invariant). Hence there exist two sets of interactions: that among q_1^i, q_2^i and q_3^i , and that between q_4^i and q_5^i . A 3×3 matrix $\{V_{jk} | j, k = 1, 2, 3\}$ can become singular at an N -fold limit point, at which $N-1$ physically independent secondary paths branch; a 2×2 matrix $\{V_{jk} | j, k = 4, 5\}$ becomes singular at a point of secondary bifurcation with N secondary paths. The same general conclusion apply for initial bifurcation in either of the modes represented by $\delta q_j^i, j = 4$ or 5 .

If the i th cell has passed the state of secondary bifurcation, its total potential energy function shows no symmetry and its incremental equilibrium equations become

$$\sum_{k=1}^5 V_{jk} \delta q_k^i - \delta_{1j} \delta P + \text{h.o.t.} = 0, \quad j = 1, \dots, 5,$$

which show an interaction among all modes $q_k^i (k = 1, \dots, 5)$. The cell in this state retains no geometric symmetry due to this interaction, and in turn cannot undergo further ‘‘symmetry-breaking’’ bifurcation. The progress of bifurcation in one cell can be understood as

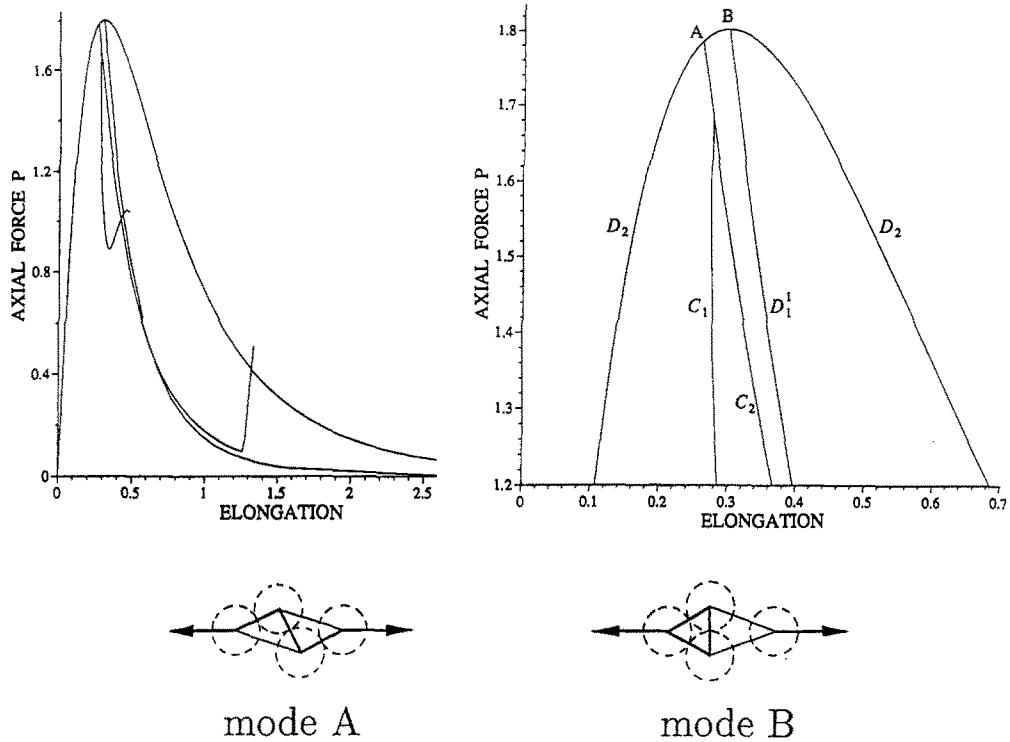


Fig. 8. End displacement $2u_1$ versus external force P relationship for the single-cell model ($n = 1$).

a process of loss of symmetry through progressive mode interaction described by the group structure shown in Fig. 5.

3.1.7. Numerical examples. Figure 8 shows end displacement $2u_1$ versus external force P relationships computed for the single-cell model ($n = 1$) under the usual Lennard–Jones assumptions for interatomic forces. The first critical point encountered on the primary path under increasing load P is the bifurcation point A , representing the C_2 -invariant shearing displacement shown as mode A. Subsequent to this and close to it appears the limit point; this occurs slightly after the Lennard–Jones relation of Fig. 4(b) reaches a maximum simultaneously in the four inclined interatomic springs. After passing this limit point and very close to it appears the bifurcation point B , and whereupon the situation is further complicated by the D_2 -invariant displacement shown as mode B.

Mode B is thus dependent on the interatomic force relation reaching a maximum, but the same does not hold for mode A. All that is required is a certain destiffening of the relation to trigger a redistribution of force within the cell. As displacement in mode A grows, the “springs” shown as light lines in Fig. 8 are loading, while those shown as heavy lines are unloading. The overall effect is that of the unloading line from bifurcation point A shown in the figure.

For the multi-cellular model ($n \geq 2$) in the absence of linking, the overall load to end-elongation relationship can be produced from that for one cell by adding end displacements of all cells for the same value of load P . This model has, irrespective of the number n , the same primary path with three n -fold compound critical points. Point A becomes an n -fold compound bifurcation, with n physically independent paths branching from the primary solution. Figure 9 shows all possible paths branching from point A for $n = 5$. The combination of the local and the global symmetries has thus realized complex bifurcation behavior. Of these possible post-critical solutions, the most likely state under real physical conditions is that lying closest to the primary path, since at sub-critical loads this has the minimum triggering energy requirement (Hunt *et al.*, 1989). We can thus conclude that without intercellular linking, the most likely failure state is one of thorough localization, in the form shown in Fig. 1(c).

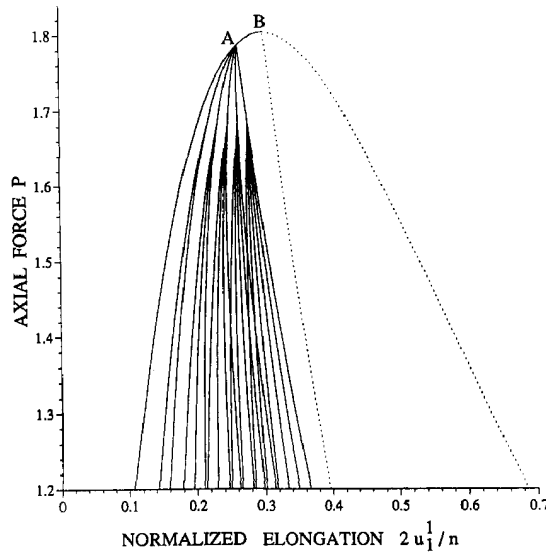


Fig. 9. End displacement $2u_1^1/n$ versus external force P relationship for the unlinked cellular model ($n = 5$).

3.2. Linked cellular model

As an example of homogeneous, distributed localization, we briefly discuss the bifurcation behavior of the weakly-linked cellular model of Fig. 1(b). In addition to the five nonlinear springs, we implement into this model three horizontal springs, which exert only small forces relative to the other five springs.

These small forces initiate interaction of energy between neighboring cells, which in turn triggers mode interaction. Off-diagonal quadratic terms appear in each of the four sets of n incremental equilibrium equations (10) and (11). The n independent equations (10) reduce to one set of equations for the primary path, characterized by a $2n \times 2n$, narrowly-banded, square block matrix for quadratic terms. The three sets of n independent equations (11) for bifurcated solutions become three sets of equations, each associated with an $n \times n$ square block matrix. Since these four block matrices in general are not identical, the eigenvalues of the linked model only have simple criticality; we note that the corresponding eigenvectors are distributed over the length. It is noteworthy that this linked model has a D_2 -invariant bifurcation structure overall due to the global symmetry, while each cell of the unlinked case has the same structure locally.

The theory with intercellular linking is most conveniently developed under a Lagrangian formalism, as with the rigid-bar model. The five fundamental degrees of freedom make this a lengthy process, and it is developed fully in a companion paper (Hunt *et al.*, 1992).

4. CONCLUDING REMARKS

The thoroughly-localized response of the unlinked atomic matrix model corresponds of course to brittle failure. Ductile behavior might reflect more the distributed form of localization, which in turn suggests intercellular linking. In the search for such solutions, described in detail in our companion paper (Hunt *et al.*, 1992), there are several pertinent conclusions that can be drawn from the single-cell behavior of Fig. 8.

The similar initial post-bifurcation slopes of the mode A and mode B responses are of immediate interest, since they are produced with the inclined "springs" in quite different states. For mode B, the limit point of the Lennard–Jones potential has been passed and all four springs are unloading, two with positive and two with negative stiffness. For mode A, on the other hand, two springs are loading and two unloading, but all at positive stiffness. This causes us to reflect on whether the sharp limit point of the Lennard–Jones law does indeed represent a true interatomic force–deflection relation; much the same response can

be produced in mode A under a gentler destiffening curve. Such a curve is adopted in our companion paper (Hunt *et al.*, (1992), largely for reasons of pragmatism since the extra instabilities of mode B and the limit point are not required for a softening overall response.

We note finally that sometimes extreme analytical care is needed. It is possible to be mesmerized by the success of periodically-based methods, such as Rayleigh–Ritz or Fourier analysis. Localized solutions are not amendable to such techniques, but are almost always accompanied by homogeneous solutions which are. Historically this seems to have led to much wasted effort, for problems in which the most likely solution is a localized one. The long axially-loaded cylindrical shell (Hunt and Lucena Neto, 1991, 1992) and the strut on a linear elastic foundation (Hunt *et al.*, 1992) are two classical examples.

Acknowledgement—The authors are grateful to Dr Kazuo Murota for his advice on the theory of this paper. This work was done at the Department of Civil Engineering of Imperial College while the first author was supported by the Japanese Ministry of Education and the second author by Calouste Gulbenkian Foundation, Lisbon.

REFERENCES

- Born, M. and Huang, K. (1954). *Dynamical Theory of Crystal Lattices*. Oxford University Press, Oxford.
- Dinkevich, S. (1991). Finite symmetric systems and their analysis. *Int. J. Solids Structures* **27**(10), 1215–1253.
- Golubitsky, M. and Schaeffer, D. G. (1985). *Singularities and Groups in Bifurcation Theory*. Vol. 1. Springer, Berlin.
- Healey, T. J. and Treacy, J. A. (1991) Exact block diagonalization of large eigenvalue problems for structures with symmetry. *Int. J. Numer. Meth. Engng* **67**, 257–296.
- Hunt, G. W. (1986). Hidden (a) symmetries of elastic and plastic bifurcation. *Appl. Mech. Rev.* **39**(8), 1165–1186.
- Hunt, G. W. (1989). Bifurcation of structural components. *Proc. Instn Civ. Engrs* **2**(87), 443–467.
- Hunt, G. W., Bolt, H. M. and Thompson, J. M. T. (1989). Structural localization phenomena and the dynamical phase-space analogy. *Proc. R. Soc. Lond. A* **425**, 245–267.
- Hunt, G. W. and Lucena Neto, E. (1991). Localized buckling in long axially-loaded cylindrical shells. *J. Mech. Phys. Solids* **39**(7), 881–894.
- Hunt, G. W. and Lucena Neto, E. (1992). Maxwell critical loads for axially-loaded cylindrical shells. *ASME J. Appl. Mech.* (to appear).
- Hunt, G. W., Providência, P. and Ikeda, K. (1992). Discrete Lagrangian theory and phase portraits for cellular structural forms.
- Hunt, G. W., Wadec, M. K. and Shicolas, N. (1992). Localized elasticae for the strut on the linear foundation. *ASME J. Appl. Mech.* (to appear).
- Ikeda, K. and Murota, K. (1991). Bifurcation analysis of symmetric structures using block-diagonalization. *Comp. Meth. Appl. Mech. Engng* **86**(2), 215–243.
- Ikeda, K., Murota, K. and Fujii, H. (1991). Bifurcation hierarchy of symmetric structures. *Int. J. Solids Structures* **27**(12), 1551–1573.
- Macmillan, N. H. and Kelly, A. (1972). The mechanical properties of perfect crystals, I. The ideal strength. *Proc. R. Soc. Lond. A* **330**, 291–308.
- Miller, W., Jr (1972). *Symmetry Groups and Their Applications*. Academic Press, New York.
- Murota, K. and Ikeda, K. (1991). Computational use of group theory in bifurcation analysis of symmetric structures. *SIAM J. Scientific and Statistical Computing* **12**(2), 273–297.
- Sattinger, D. H. (1979). *Group Theoretic Methods in Bifurcation Theory*. Springer, Berlin.
- Thompson, J. M. T. and Hunt, G. W. (1973). *A General Theory of Elastic Stability*. Wiley, New York.
- Thompson, J. M. T. and Hunt, G. W. (1984). *Elastic Instability Phenomena*. Wiley, New York.
- Thompson, J. M. T. and Shorrock, P. A. (1975). Bifurcation instability of an atomic lattice. *J. Mech. Phys. Solids* **23**(21), 21–37.